



In vitro release and cytotoxicity activity of 5-fluorouracil entrapped polycaprolactone nanoparticles

Moshera Samy¹ · Heba M. Abdallah¹ · Hanem M. Awad² · Magdy M. H. Ayoub¹

Received: 4 October 2020 / Revised: 24 May 2021 / Accepted: 22 June 2021 /
Published online: 27 July 2021

© The Author(s), under exclusive licence to Springer-Verlag GmbH Germany, part of Springer Nature 2021

Abstract

In this study, 5-fluorouracil (5-FU) entrapped polycaprolactone nanoparticles (5-FU-PCNPs) have been prepared using double emulsion method. The different factors were examined for assembly to arrive at the best effective formulation of 5-FU-PCNPs formulation for 5-FU-PCNPs, as polymer concentration, stabilizer concentration. The encapsulation efficiency of PCNPs was in the range of 18.8–45.4%. The prepared nanoparticles showed the spherical shape having an average size of 183–675.5 nm, whereas TEM exhibited the prepared nanoparticles have a spherical shape. FTIR, XRPD, confirmed successful insertion of drug in prepared PCNPs. In vitro release of 5-FU from selected formulations showed sustained release from the nanoparticles where slower release was observed when lower PVA concentration was used. Anticancer activity was examined against cell culture for HCT-116 (human colorectal carcinoma), MCF-7 (human breast adenocarcinoma), HepG2 (human hepatocellular carcinoma) and A549 (human lung carcinoma) for six formulations 5-FU-PCNPs nanoparticles. The in vitro cytotoxic activity of the prepared formulations was tested showing that these formulations appeared as promising active anticancer formulations.

Keywords Polycaprolactone · 5-Fluorouracil · Double emulsion · HCT-116 · MCF-7 · HepG2 · A549 · Cytotoxicity

✉ Moshera Samy
moshera_samy1984@yahoo.com

¹ Polymers and Pigments Department, National Research Centre, Dokki, Giza 12622, Egypt

² Tanning Materials and Leather Technology Department, Centre of Excellence, National Research Centre, Dokki, Giza 12622, Egypt

Introduction

Cancer nanotechnology is an interdisciplinary area of research in science, engineering and medicine with a broad applications for molecular imaging, molecular diagnosis and targeted therapy [1, 2]. During the past decade, several research articles have been published that present smart particle systems for delivering nanodrug systems for specific methods to improve tumor treatment and imaging as many reviews have attempted to describe and classify these NPs [3, 4]. They all approved to define systems such as nanocomposites capable of incorporating drug and contrast agent (s) and could be either nanocarriers or nanovectors [5]. It specifically consisted of a scaffold made primarily of a corona of polymers capable of improving the many biopharmaceutical and pharmacological properties of entrapped drugs. They can also have a binding compound on their surfaces that provides aiming for a specific cancer biomarker expressed in specific cancer cells [6]. 5-Fluorouracil (5-fluoro -2, 4-pyrimidinedione, 5-FU) is pyrimidine antimetabolite. It is used as an anti-tumor agent to treat multiple solid tumors in the liver, kidney, ovaries, breast, pancreas, stomach, head, brain and neck [7–10]. 5-FU is listed by the World Health Organization (WHO) among the most important drugs required in a basic health system [11]. Because of its structure, 5-FU can be entrapped into DNA and RNA. It can moreover impede the metabolism of nucleosides, which leads to finally cell death and cytotoxicity [12]. The main drawbacks of using 5-FU have lack of specificity leading to systemic toxicity, extremely low bioavailability and short plasma half-life. This results in the use of high doses, resulting in side effects and thus multiple adverse effects such as diarrhea, severe anemia and vomiting [13–15]. The improvement of resistance by cancer cells has also greatly limited the clinical applications of 5-FU [16, 17]. One of the solutions to beat this shortcoming is 5-FU incorporation into polymeric nanoparticles. These drug delivery carriers have unique properties such as the ease of modifying their surface properties, the capability to increase drug stability and protect the drug entrapped [18]. The nanoparticles are not rapidly cleared and accumulate in the tumor interstitium. This is known as enhanced permeability and retention (EPR) effect, a tumor property that Matsumura and Maeda exploited [19] as a mean to goal anticancer agents for solid tumors. Biodegradable polymeric nanoparticles can moreover increase drug bioavailability, provide a controlled pattern of drug release and improve cell and tissue selectivity [20]. In recent years, there has been a significant increase in interest in investigating in the field of drug delivery. Nanoparticulate drug carriers can be formulated using some kinds of polymers. They have the ability to include different classes of chemotherapy agents, thus keeping them from protein absorption, non-specific absorption of major organs and renal clearance. A selection of biodegradable polymers has been studied for possible use as drug delivery nanocarriers. It is careful to be an effective controlled drug delivery system [21]. Biodegradable polymeric nanoparticles (PNPs) are solid carriers described with sizes less than 1 μm that have the ability to drug entrapment into their polymeric matrix [22, 23]. In addition, some reports have shown that these nanocarriers can

modify the *in vitro* drug release profile by changing the molecular weight and degradation rate of polymers used in their formulation [24, 25]. Polycaprolactone (PCL) has been preferred as a valuable biodegradable polymer for the preparation of PNPs as it is used in several medicinal applications due to its high degree of crystallinity, biodegradability, hydrophobicity, biocompatibility, safe properties and its ability to protract drug time at the target locations [26]. PCL nanoparticles (PCNPs) were prepared by the double emulsion which is commonly used to load both lipophilic and hydrophilic materials into a complex heterogeneous dispersed system called "emulsion" [27, 28]. Consequently, the present work aims to study the various factors that influence both the formation of 5-FU-loaded PCNPs and their efficiency as a 5-FU carrier. The effect of factors as: (1) the effect of the PCL concentration of the first emulsion and (2) the concentration of the stabilizer concentration of the second emulsion of the emulsification process on the suspension properties of the nanoparticles. Also, the drug encapsulation efficiency (EE%) and particle size (PS) were also examined for the prepared particles. Also, drug crystallization in 5-FU-PCNPs and the interaction between 5-FU and chitosan were evaluated by XRD, FTIR, TEM and SEM. It was examined and studied for its cytotoxic activity against HCT-116, MCF-7, HepG2 and A549.

Experimental

Materials

Polycaprolactone (PCL; $C_6H_{10}O_2$; $M_w = 14,000$ g/mol), polyvinyl alcohol (PVA; $M_w = 30,000$ g/mol; 87–89% hydrolyzed; m.p. 200 °C), dichloromethane (DCM) and 5-Fluorouracil (5-FU; $C_4H_3FN_2O_2$; 5-Fluoropyrimidine-2, 4-dione, $\geq 99\%$) were delivered from Sigma-Aldrich, Germany. Acetic acid (CH_3COOH) was obtained from SHAM laboratory chemical; acetic acid is of pure grades. All other chemicals—otherwise mentioned were provided from Sigma-Aldrich, Germany, and were used as received.

Methods

Preparation of 5-fluorouracil loaded polycaprolactone nanoparticles (5-FU-PCNPs)

The biodegradable nanoparticulate systems were attained by loading the active anti-cancer drug (5-FU) into PCL (oil phase), which was encapsulated by PVA (water phase, W1) acting as the polymer emulsifier (stabilizer) [27, 29].

Preparation of polyvinyl alcohol (PVA) solution To be used as emulsion stabilizer in outer aqueous phase, two PVA stock solutions (0.5% and 1 wt. % stocks A and B) were prepared by slowly adding 2.5 mg and 5 mg PVA, respectively, into 500 mL distilled water with stirring and heating at 60 °C for 40 min to obtain a clear 0.5% PVA solution.

Preparation of primary emulsion (First step) In the first step, in order to make the primary emulsion (W1/O), stock solutions of 1%, 2% and 3 wt.% PCL (stocks A, B and C, correspondingly) were prepared by slowly adding of 1.05 g, 2.10 g and 3.15 g PCL, respectively, into 100 mL DCM until fully dissolved with stirring till forming a clear solution. 10 mg of 5-FU was dissolved in 1 ml of 0.5% acetic acid in order to aid the dissolution of 5-FU, and then, 5 ml PCL solution was added. This mixture was properly homogenized using digital high speed homogenizer (T-10; model) at 20,000 rpm for 5 min using to have the first emulsion (W1/O) [31].

Preparation of double emulsion (second step) In the second step, the primary emulsion (W1/O) was added in the outer aqueous phase (W2) containing stocks (A, and B) PVA solutions as stabilizer with homogenization to achieve the double emulsion W1/O/W2 [29, 30]. This mixture was properly homogenized at 21,000 rpm for 15 min by using digital high speed homogenizer (T-10; model). In second step, we used excess of outer aqueous phase (W2) in order to facilitate the diffusion of organic solvent from PCL particle to outer aqueous phase. The obtained double emulsion ($W_1/O/W_2$) was subjected to evaporation under vacuum using rotary evaporator (Heidolph type VV2000, type WB2000, Germany) until the whole organic solvent (DCM) was removed [31]. The nanoparticles were collected and separated from the free drug in the nanoparticulates' suspension by centrifuge (Ambient centrifuge centurion scientific model: K2015, UK) at 6000 rpm for 45 min. Then, the produced nanoparticles' pellets were washed two times with ultra-pure water. The supernatant solution was used for determination of the drug encapsulation efficiency. The supernatant solution was used for determination of drug encapsulation efficiency. The supernatant was kept for drug assay as described later and the precipitate was lyophilized using freeze-dried, and the powder was used for further analyses. Drug-free nanoparticles (PCNPs) were prepared by the same way using only the 0.5% acetic acid solution.

Method of 5-fluorouracil (5-FU) analysis

Determination of λ_{\max} of 5-FU

The spectrophotometric assay adopted for 5-FU analysis by screening of 5-FU in the investigated solvent such as 0.5% acetic acid and phosphate buffer solution (PBS) using (Shimadzu UV spectrophotometer, 2401/PC, Japan) through a scan range of 200–400 nm. The 5-FU dissolved in investigate solvent at 10 $\mu\text{g}/\text{ml}$ was screened in order to determine the λ_{\max} of 5-Fluorouracil from UV spectrum, using investigated solvent as a blank. This concentration was prepared by dilution from dilution of a stock solution of (10 $\mu\text{g}/\text{ml}$) which was prepared by dissolving 10 mg of 5-FU, accurately weighed, in 10 ml investigate solvent.

Establishment of the standard curve of 5-FU

Six concentrations of 5-FU in investigate solvent were prepared by using appropriate dilutions of stock solution previously mentioned, six concentrations of 5-FU,

dissolved in investigate solvents such as 0.5% acetic acid and phosphate buffer solution (PBS), were prepared. The concentrations prepared were 4, 6, 8, 10, 12, 14 and 16 $\mu\text{g/ml}$. The absorbance of each of these concentrations was recorded at the λ_{max} recorded using investigate solvent as a blank. A linear curve was plotted relating concentration of 5-FU and the UV absorbance at the relevant wavelength of maximum absorption of 5-FU in the investigated solvent.

In vitro anticancer activity

Cell culture of HCT-116 (human colorectal carcinoma), MCF-7 (human breast adenocarcinoma), HepG2 (human hepatocellular carcinoma), A549 (human lung carcinoma) and RPE-1 (human normal retina pigmented epithelium) cell lines were purchased from the American Type Culture Collection (Rockville, MD) and maintained in DMEM medium which was supplemented with 10% heat-inactivated FBS (fetal bovine serum), 100 U/ml penicillin and 100 U/ml streptomycin. The cells were grown at 37 °C in a humidified atmosphere of 5% CO_2 .

MTT anticancer assay

The anticancer activities against HCT-116, A549, HepG2 and MCF-7 human cancer cell lines as well as on RPE-1 human normal cells were estimated using the 3-[4,5-dimethyl-2-thiazolyl)-2,5-diphenyl-2H-tetrazolium bromide (MTT) assay, which is based on the reduction of the tetrazolium salt by mitochondrial dehydrogenases in viable cells [32–34]. Cells were dispensed in a 96-well sterile microplate (5×10^4 cells/well) and incubated at 37 °C with series of different concentrations, in DMSO, of each tested compound or doxorubicin (positive control) for 48 h in a serum-free medium prior to the MTT assay. After incubation, media were carefully removed, 40 μL of MTT (2.5 mg/mL) was added to each well and then incubated for an additional 4 h. The purple formazan dye crystals were solubilized by the addition of 200 μL of DMSO. The absorbance was measured at 570 nm using a Spectra Max Paradigm Multi-Mode microplate reader. The relative cell viability was expressed as the mean percentage of viable cells compared to the untreated control cells. All experiments were conducted in triplicate and repeated on three different days. All the values were represented as mean \pm SD. IC_{50} s were determined by probit analysis by SPSS Incprobit analysis (IBM Corp., Armonk, NY, the USA).

Characterization of 5-FU-loaded PCNPs

Determination of encapsulation efficiency In order to determine the EE% of 5-FU in the prepared nanoparticles, the combined washings after centrifugation were appropriately diluted using 0.5% acetic acid. The amount of free, unencapsulated 5-FU was measured spectrophotometrically at 265.2 nm using the regression equation of the standard calibration curve plotted employing suitable concentrations of 5-FU [35]. The amount of encapsulated 5-FU was determined by difference between the amount

of free, unencapsulated 5-FU in the combined washings and the initial amount used in preparation of PCNPs where the following equation was employed [36, 37]:

$$EE\% = \frac{\text{Freedrug} - \text{Totaldrug}}{\text{Totaldrug}} \times 100 \quad (1)$$

Determination of particle size (PS) The PS for the prepared nanoparticles was measured by means of photon correlation spectroscopy (PCS) using a Zeta-sizer (Nano ZS, Malvern Instruments Ltd., Malvern, the UK). Samples were suitably diluted with distilled water and measured at ambient temperature using quartz cuvettes.

Fourier transform infrared spectroscopy FTIR spectroscopy was used to study the chemical composition of PCL, 5-FU, PVA as well as the selected 5-FU-loaded PCNPs. The spectra were recorded using FTIR spectrometer (Jasco, FT/IR 6100, Japan). The KBr pellet method was employed where the powdered samples were ground and mixed with KBr then compressed into disks. To collect the data for each spectrum, 32 scans were performed in the mid-infrared range 4000–400 cm^{-1} .

X-ray powder diffraction (XRPD) The physical state of 5-FU, PCL, PVA and selected 5-FU-loaded PCNPs formulations was evaluated using XRPD. Measurements were acquired with X-ray diffractometer (Bruker AXS, D8 Advance, Germany) which was operated at 40 kV and 40 mA using $\text{CuK}\alpha$ as a radiation source where $\lambda = 1.54 \text{ \AA}$. The diffractograms were recorded in the diffraction angle (2θ) range between 4° and 50° , and the process parameters were set at scan step size of 0.020° and scan step time of 0.4 s.

Thermal analysis (TA) Thermal analysis is useful for evaluating thermal properties and drug–polymer interactions to assess the influence of recipients and micro- or nano-encapsulation process on the physicochemical characteristics of the pharmaceutical materials. Differential scanning calorimetry (DSC) and thermal gravimetric analysis (TGA) are the most frequently used thermo-analytical techniques [38].

Differential scanning calorimetry (DSC). Thermal stability of freeze-dried 5-FU–PCNPs was investigated through DSC using thermal analyzer DSC–SDT (Simultaneous DSC-TGA) Q600 V20.9 Build 20, the USA, in the range from room temperature to 500°C at a heating rate of $10^\circ\text{C}/\text{min}$ under inert nitrogen atmosphere (N_2) using reference alumina. The samples weight was between 2.5 and 12 mg.

Thermal gravimetric analysis (TGA) Thermal behavior for freeze-dried 5-FU–PCNPs samples was recorded using thermal analyzer TGA–SDT Q600 V20.9 Build 20, (USA) in the range from room temperature to 700°C at a heating rate of $10^\circ\text{C}/\text{min}$ under inert nitrogen atmosphere (N_2) using reference alumina.

Transmission electron microscopy The morphology of a selected 5-FU-loaded PCNPs formulation and their dimensions in nanometer range was confirmed by transmission electron microscopy. The TEM (JEOL Co., JEM-2100, Japan) was adjusted at a high tension electricity of 200 kV. One drop of the appropriately diluted sample

was placed onto a carbon-coated copper grid, negatively stained with 1% phosphotungstic acid and left to dry at ambient temperature before being examined at suitable magnifications.

Scanning electron microscopy (SEM) The morphology of the prepared freeze-dried nanoparticles was investigated by scanning electron microscopy (SEM) using Quanta FEG 250 (FEI Company, Holland) device. Freeze-dried nanoparticles were deposited on a flat aluminum holder and were dried at room temperature. The concerned sample in each case was finally coated under vacuum by cathodes sputtering with gold for 3 min.

In vitro drug release study

The in vitro release of 5-FU, in free form and from selected prepared PCNPs, was evaluated employing the dialysis bag technique [39] employing a dialysis tubing cellulose membrane (Visking®, SERVA Electrophoresis GmbH, Germany; Molecular weight cutoff 12.000–14.000). An amount equivalent to 2 mg of 5-FU was instilled in the dialysis bag, sealed at both ends to prevent leakage and placed in screw-capped glass containers filled with 100 ml phosphate buffer (pH 7.4). The entire system was kept at 37 ± 0.5 °C at 100 rpm using a shaking water bath. At predetermined time intervals (1, 2, 3, 4, 6, 8, 24 and 48 h), 5 ml of the release medium was withdrawn and replaced with 5 ml of fresh buffer solution. The samples were adequately diluted and analyzed for 5-FU content spectrophotometrically at 266.4 nm [40]. The cumulative percentage of drug released was determined as the ratio of the amount of released 5-FU to the amount of 5-FU initially inserted into the dialysis bag. All measurements were performed in triplicates.

Statistical analysis

Results are presented as mean \pm SD. Statistical analysis was performed by means of one-way analysis of variance (ANOVA). All experiments were repeated at least three times. All data were expressed as means \pm standard deviations of sample means. The statistical significance of the differences was evaluated by one-way analysis of variance and $P < 0.05$ was considered to indicate a statistically significant difference.

Results and discussion

Preparation of PCNPs and 5-FU-PCNPs

PCNPs and 5-FU-PCNPs were synthesized by double emulsification method. Various factors were studied such as different concentrations of PCL (1%, 2%, and 3%) according to the literature [31, 41], respectively, and different concentrations of PVA (0.5% and 1%) for second emulsion were investigated. Double emulsion was prepared by two-step emulsification process using polyvinyl alcohol as stabilizer where PVA is the most widely used stabilizer due to good solubility in water,

its availability in a wide range of molecular weights and low toxicity [42]. Also, a stable double emulsion was obtained using homogenization speeds of 20,000 rpm at 5 min for the first emulsion and 21,000 rpm at 15 min for the second emulsion selected to prepare the PCNPs providing the lowest particle size [29]. In the second emulsion step, excess external aqueous phase (W2) was used to facilitate diffusion of dichloromethane from the PCL particles to the external aqueous phase. The effect of different factors on the properties of the nanoparticles prepared by double emulsification was studied by keeping constant the PCL concentrations (1%, 2%, 3%) at a 5 min stirring time at the stirring speed of 20,000 rpm for the first emulsion where two different concentrations of PVA were tested as being (0.5% and 1%) stirring time is 15 min at 21,000 rpm as constant stirring speed of the second emulsion as shown in Table 1.

The assay of 5-fluorouracil (5-FU)

The assay of 5-FU wavelength of maximum absorption (λ_{\max}) started by screening of 5-FU in two solvents such as 0.5% acetic acid and phosphate buffer saline (PBS).

Method of 5-FU analysis in 0.5% acetic acid

Determination of λ_{\max} of 5-FU The determination of 5-FU λ_{\max} wavelength started by screening of 5-FU in 0.5% acetic acid through a scan range of 200–400 nm where the λ_{\max} . The UV spectrum of 5-FU in 0.5% acetic acid is shown in Fig. 1. The concentration used for this spectrum was 10 $\mu\text{g/ml}$.

Table 1 EE% and PS values of investigated of 5-FU–PCNPs formulations

Formulations*	First emulsion factors PCL Conc. (%) **	Second emulsion factors PVA Conc. (%) ***	EE% \pm SD	PS (nm) \pm SD
F 15	1	0.5	34 \pm 9.41	239.4 \pm 28.3
F 11		1	20.5 \pm 11.32	675.5 \pm 62.4
F _B				1178 \pm 232.5
F 25	2	0.5	45.4 \pm 0.93	509.2 \pm 82.4
F 21		1	29 \pm 0.64	465.6 \pm 76.1
F 35	3	0.5	18.8 \pm 7.65	485.6 \pm 65.5
F 31		1	40.7 \pm 6.81	183 \pm 23.7

F_B is the prepared polymeric nanoparticles free from 5-FU at concentration of PCL for first emulsion–1 wt. %, and concentration of PVA for second emulsion–1 wt. %.

*All samples were prepared using 10 mg/ml of 5-FU at 20,000 rpm as homogenization speed for the first (for 5 min) and at 210,000 rpm second emulsion (for 15 min), respectively

**Samples containing first numbers 1–3 refer to a concentration of PCL for first emulsion as 1%, 2% and 3 wt. %, respectively

***Samples containing second numbers 0.5–1 refer to a concentration of stabilizer PVA for second emulsion as 0.5% and 1%, respectively

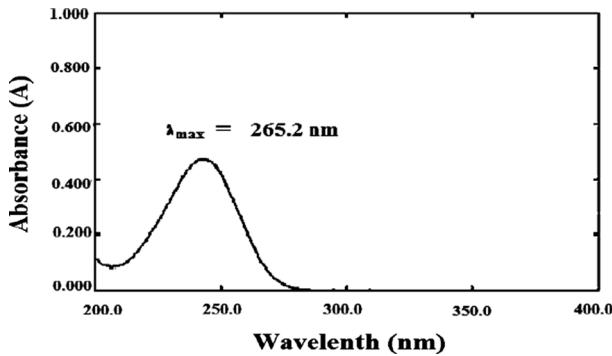


Fig. 1 UV spectrum of 5-FU in 0.5% acetic acid at $\lambda_{max} = 265.2 \text{ nm}$

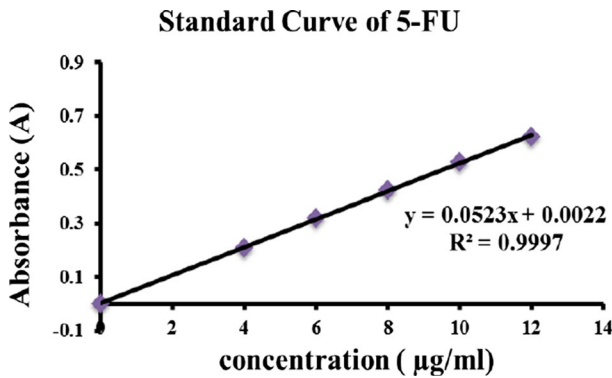


Fig. 2 Standard curve of 5-FU in 0.5% acetic acid

Establishment of the standard curve of 5-FU Five concentrations of 5-FU in 0.5% acetic acid were prepared by dilution of stock solution of 10 µg/ml. These concentrations were 4, 6, 8, 10 and 12 µg/ml. The absorbance of each of these concentrations was recorded at the wavelength of maximum absorption λ_{max} 265.2 nm previously recorded using 0.5% acetic acid as a blank [35, 40]. Standard curve was plotted Fig. 2 shows that a linear relationship was established between concentration of 5-FU and UV absorbance where regression equations ($y = 0.0523x + 0.0022$) and the linear regression with correlation coefficient ($R^2 = 0.9997$) proving the efficacy and reliability of assay for determination of 5-FU concentration. The slope was calculated and was found to be 0.0523.

Method of 5- fluorouracil analysis in phosphate buffer saline (PBS)

The determination of wavelength of maximum absorption (λ_{max}) of 5-FU started by screening of 5-FU in PBS at PH 7.4 through a scan range of 200–400 nm where the

λ_{\max} was determined. Six concentrations of 5-FU were prepared, and the absorbance of each of these concentrations was recorded at the λ_{\max} relevant to the used solvent Fig. 3.

Determination of λ_{\max} of 5-FU in PBS The determination of 5-FU λ_{\max} wavelength started by screening of 5-FU in PBS at PH 7.4 through a scan range of 200–400 nm where the λ_{\max} . The UV spectrum of 5-FU in PBS at PH 7.4 is shown in Fig. 3. The concentration used for this spectrum was 10 $\mu\text{g/ml}$.

Establishment of the standard curve of 5-FU in PBS Six concentrations of 5-FU in PBS at PH 7.4 were prepared by dilution of stock solution of 10 $\mu\text{g/ml}$. These concentrations were 4, 6, 8, 10, 12 and 14 $\mu\text{g/ml}$. The absorbance of each of these concentrations was recorded at the λ_{\max} 266.4 nm previously recorded using PBS at PH 7.4 as a blank [40]. Standard curve was plotted (Fig. 4) and shows that a linear relationship was established between concentration of 5-FU and UV absorbance where the regression equations ($y=0.0451x+0.003$) and the linear regression with correlation coefficient $R^2=0.998$ proving the efficacy and reliability of assay for determination of 5-FU concentration. The slope was calculated and was found to be 0.0451.

Encapsulation efficiency (EE%)

EE% means that the amount of 5-FU administered in the particles at the end of the procedure. Therefore, EE% depends on several factors associated with polymer concentration, drug, [43, 44], stabilizer concentration, emulsion technique (i.e., stirring speed and time) and additives in the inner and outer water phase [44]. Table 1 shows the amount of EE%, PS of 5-FU-PCNPs prepared using a different PCL concentrations of the first emulsification step. The obtained results indicated that all the obtained formulations showed EE% values ranged from 18.8 to 45.4%. Table 1 shows that increasing the PCL concentration of the first emulsion (1–2%), with a constant concentration of stabilizer (PVA, 1%) and with keeping the other parameters constant for the first and second emulsion (F11; F21; F31), there was a general increase in the efficiency of the observed the EE% values with increasing

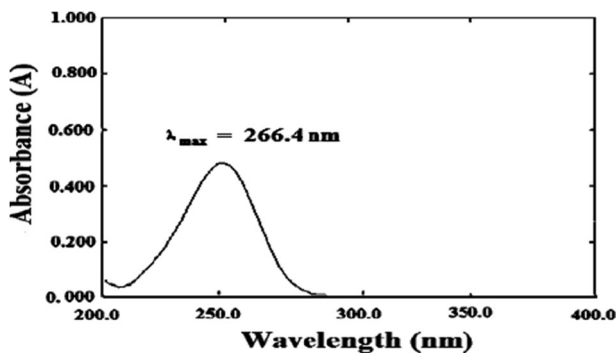


Fig. 3 UV spectrum of 5-FU in PBS at PH 7.4

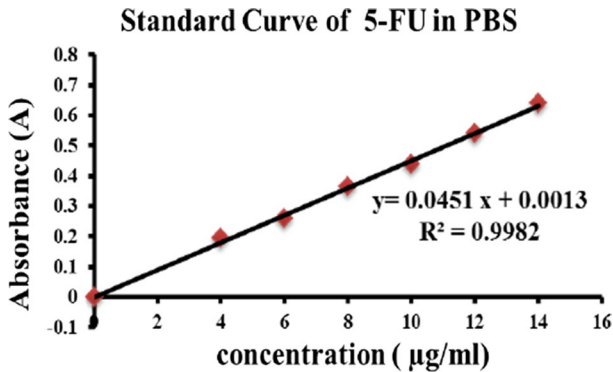


Fig. 4 Standard curve of 5-FU in PBS at PH 7.4

PCL concentration (from 20.5% for F11 to 29% for F21, and to 40.7% for F3: 1). Similar results were recorded by increasing the PCL concentration of the first emulsion (1–2%), at constant concentration of stabilizer (PVA, 0.5%) such as (F15–F25), there was a general increase in EE% values, observed with increasing PCL concentration (from 34%; F15 to 45.4; F2: 0.5), respectively. It was found that decrease in EE% values was observed with increasing stabilizer (PVA) concentration of second emulsion at constant concentration of PCL of first emulsion (1%), keeping the other factors constant for the first and second emulsion (F15; F11) (i.e., from 34%; F15 to 20.5%; F11). A clear increase in the encapsulation efficiency (EE %) values was observed with increasing concentration of PVA (from 20.5%; F11 to 23.1%; F12). Similarly, increasing the stabilizer PVA concentration of second emulsion at constant concentration of PCL of first emulsion (2%), keeping the other factors constant for the first and second emulsion (F20.5–F21) has led to increase in EE% values observed with increasing concentration of PVA (from 29%; F20.5 to 45.4%; F21). In conclusion, the encapsulation efficiency increased with increasing PVA concentration. EE% is presented in Fig. 5.

Particle size (PS)

PS is an important factor, which influences the pharmaceutical characteristic of the carrier. Hence, the particles size is evaluated as a function of formulation factors. Accordingly, the particles sizes for the prepared nanoparticulates formulations were determined as shown in Table 1. The PS of PCNPs having an average size of 183–675.5 nm. An increase in the particles size of the formulations with increasing the concentration of PCL of first emulsion, keeping both the concentration of PVA for second emulsion (0.5%), and the other factors constant for the first and second emulsion (F15; F25). Particle size values of the prepared (5-FU-PCNPs) observed until concentration of PCL (from 239 nm; F15 to 509.5 nm; for F25). A clear decrease in the values of particle size of the prepared (5-FU-PCNPs) was observed with increasing concentration of PCL (from 509.5; for F25 to 485.6 nm; for F35). A clear decrease in the particle size values was observed with increasing

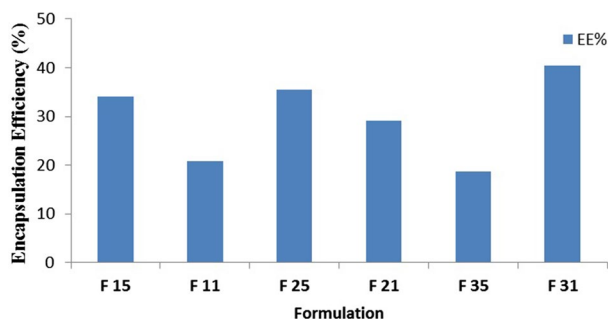


Fig. 5 Encapsulation efficiency (EE, %) of 5-FU–PCNPs formulations. The error bars correspond to standard deviations of triplicate formulation

PCL concentration (from 509; F25 to 239 nm; F21). The particles size of the prepared 5-FU-PCNPs increased. According to Ortiz et al. [45], by increasing concentration of PCL of first emulsion. This was in fine agreement with our findings where, for example, it was found that by increasing concentration of PCL for first emulsion, a remarkable decrease in the particle size value was observed. However, at higher concentration of PCL of the first emulsion (i.e., 2% and 3%), the particle size increased which could be attributed to possible particle aggregations. We find that the particles size decreased with increased the PVA concentrations of second emulsification from 0.5 to 1%, at constant the other factors constant including the factors in case of F2:0.5–F2:1, a particles size of 509.2 nm at 0.5% PVA, whereas in case of F25, the particle size was reduced to 239 nm in case of F21. A decrease in particles size agrees with the results obtained by Ozturk et al. [46]. However, a very slight increase was observed in particle size at concentration of PVA (3%), and the particles size increased which due to possible collections of obtained particles. The results reported were agreed with the literature as the stabilizer concentration is a major factor in determining the particle size prepared by double emulsion method [30, 46] whereby increasing the stabilizer concentration in the second emulsion, the particles size was reduced. While polyvinyl alcohol has a high molecular weight polymer, the presence of PVA in most of the outer phase of the water can increase the viscosity of the diffusion phase, making it more difficult to reduce the emulsion particles to a smaller size [30]. Also, it was found that the particles size of the prepared PCNPs without 5-FU (F_B ; 1178 nm) is high as compared with the prepared 5-FU-PCNPs (F31; 500.5 nm) which were prepared at 3% concentration of PCL of first emulsion and 1% of PVA of second emulsion. That means that the drug entrapment of 5-FU into the prepared PCNPs will affect the particles size.

FTIR characterization

The FTIR spectra were represented as in Fig. 6 and Table 2. Table 2 indicated the specific peaks of PVA, 5-FU, PCL and 5-FU–PCNPs formulations (F11, F21 and F31), respectively. Specific peaks for PCL appeared at 1636.3 and 1729.8 cm^{-1} which were reported in the expansion carbonyl vibration of bonds

[47]. The specific bands of pure 5-FU appeared in 1725.01, 1426, 1245.7, 809.9 and 546.7 cm^{-1} due to imide vibration (amide II and amide III) and the aromatic ring, 1348 cm^{-1} related to the pyrimidine ring vibration, 1179.2 cm^{-1} due to C=O, and 1245.7 cm^{-1} related to vibrations of CN [48]. Broad spectrum between 3500 and 3000 cm^{-1} is noticed, which is associated with the stretching of the –NH vibration. Whereas the spectra of 5-FU-PCNPs formulations have presented peaks at 1632.4 and 1729.8 cm^{-1} were due to the absorption of the carbonyl and residual acetate groups. The weak peak at 1467.5 cm^{-1} showed the presence of CH₂. The FTIR spectra presented the specific mid and weak peaks of 5-FU-PCNPs at 2947.6 and 2867.6 cm^{-1} that were associated with vibration of asymmetric and C-H, respectively. A weak peak of 1470.4 cm^{-1} was indicated to the bending CH₂ band. That peak presented a physical interaction between 5-FU and PCL as well as the spectrum of the 5-FU-PCNPs formulations that maintained

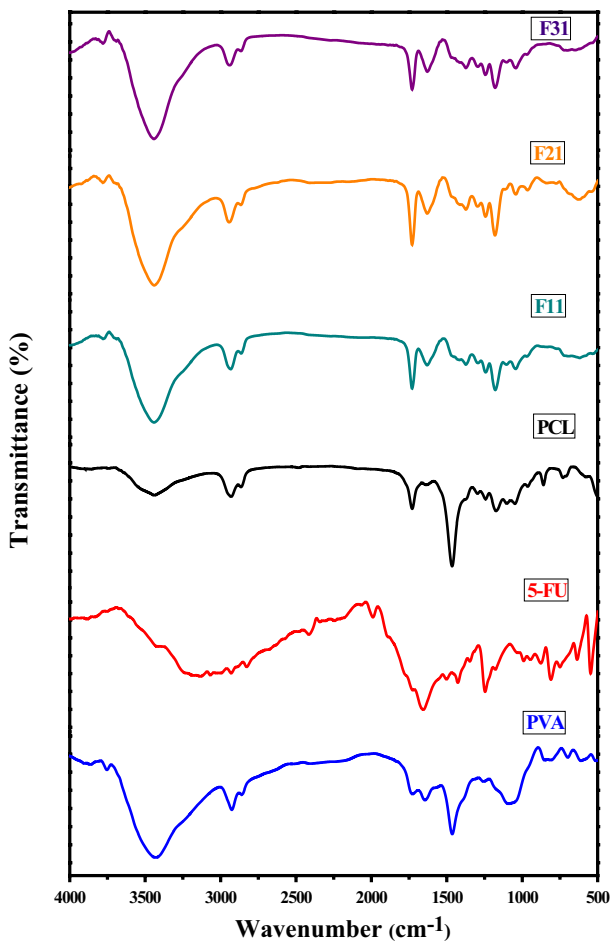
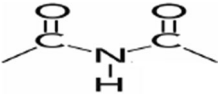
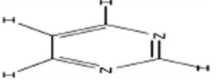


Fig. 6 FTIR spectra of PVA, pure 5-FU, PCL and 5-FU-PCNPs for (F11, F21 and F31), respectively

Table 2 FTIR peak assignments for pure 5-FU, PCL and 5-FU-PCNPs

Type of polymer	Wave number (cm ⁻¹)	Vibration type	Abbreviation
PCL	1729.8	Carbonyl stretching vibration	$\nu_{as}(C=O)$
5-FU	1725.01	Carbonyl stretching vibration	$\nu_{as}(C=O)$
	1725.01, 1426, 1245.7, 809.9, and 546.7 cm ⁻¹	Imide vibration (amide II and amide III)	
	1348	Pyrimidine ring vibration	
	1179.2	Carbonyl vibration	C=O
	1245.7	CF stretching band	CF
	3000–3500	–NH stretching vibration	–NH
5-FU-PCNPs	1632.4	Carbonyl vibration	C=O
	1729.8 cm ⁻¹	Residual acetate vibration	
	1467.5	CH ₂ vibration	CH ₂
	2947.6	Asymmetric C–H stretching	C–H
	2867.6	Symmetric C–H stretching	C–H

the highest specific peaks for 5-FU with a slight shift and confirmed drug entrapment by PCNPs.

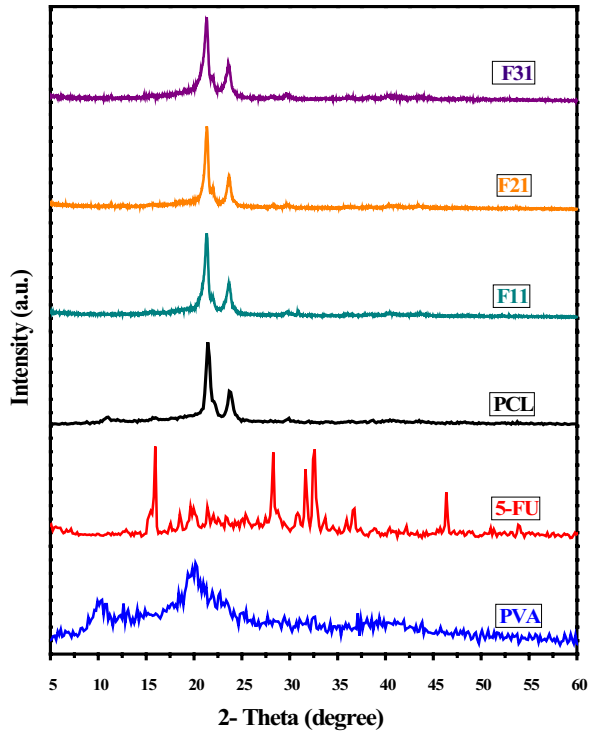
XRPD

The XRPD patterns of PVA, 5-FU and pure PCL samples are represented in Fig. 7. PCL showed two sharp peaks that were mentioned to scattering from crystalline phase [45]. Pure 5-FU displays multiple sharp peaks representing the highly crystalline nature of the 5-FU [45]. PVA showed two diffuse reflections and several low intensity reflections revealing its amorphous nature. Figure 7 represents the XRPD patterns for the three 5-FU-loaded PCNPs formulations as shown in Table 1 by making the first and second emulsion at different concentrations of PCL. Two peaks due to the crystalline phase of PCL, while the well-known specific peaks of 5-FU disappeared indicate that 5-FU molecules were distributed at the molecular level in the matrix PCL as reported in the literature [49, 50].

Thermal analyses

Both TGA and DSC techniques usually provide qualitative and quantitative information about the thermal properties of the nanoparticles.

Fig. 7 XRPD patterns of PVA, 5-FU, PCL and 5-FU-PCNPs formulation (F11, F21 and F31), respectively



DSC

Differential scanning calorimetry is essentially used to measure enthalpy changes according to the changes in the thermal properties of the material as a function of time or temperature. The final melting temperatures and enthalpy changes were elucidated from DSC thermograms as indicated in Fig. 8. Pure PCL showed $T_m = 60.66$ °C, while T_m of PVA recorded at 290.52 °C. The DSC curve of 5-FU exhibits endothermic peak at the temperature of 282.80 °C corresponding to its melting point [51]. The recorded T_m of PCL was nearly similar to the reported theoretical value [51] which confirmed that the crystallization and the melting behavior of PCL were not changed by the double emulsion method [52]. DSC thermograms of different samples of 5-FU-PCNPs as shown in Fig. 8 revealed disappearance of the distinguished endothermic peak for 5-FU at $T_m = 282.80$ °C. Therefore, 5-FU-PCNPs demonstrated molecularly dispersed drug in the nanoparticles as previously mentioned in the literature [53].

TGA

Thermal gravimetric analysis normally provides information on mass loss as a function of temperature. TGA thermograms of pure PCL, PVA, 5-FU and 5-FU-PCNPs (F11, F21 and F31) were represented as shown in Fig. 8. PCL was thermally

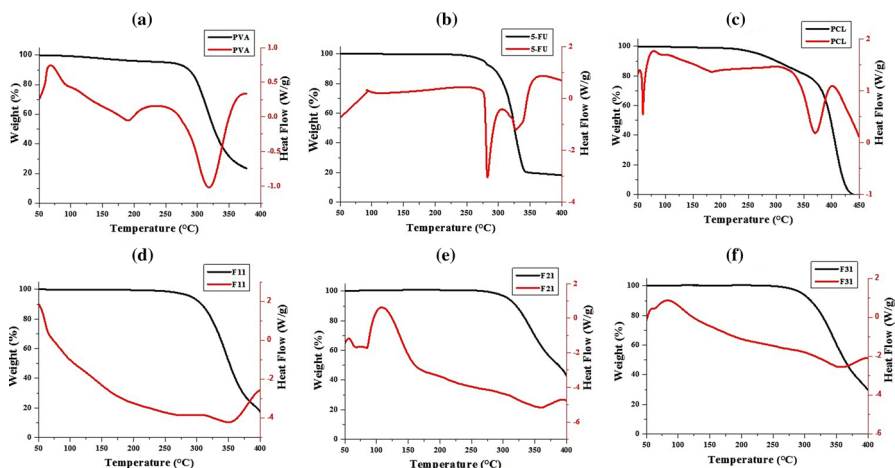


Fig. 8 DSC and TGA thermograms of **a:** PVA, **b:**5-FU, **c:** PCL and **d, e** and **f:**5-FU-PCNPs formulation (F11, F21 and F31), respectively

stable until 270 °C where the thermal decomposition occurred in two steps at 250 and 380 °C with weight loss of 20 and 60%, respectively. Thermal degradation of PVA decomposed at 275 °C due to the rupture of the polyester chains via ester pyrolysis reaction with the release of CO₂, H₂O, and formation of carboxylic acid groups according to Fukushima et al. [52]. On the other hands, thermal decomposition of 5-FU occurred in two steps. The degradation step takes place in the range of 280–340 °C with weight loss of 10, 86%, respectively, due to the loss of water. Also, it was noticed that all formulations of 5-FU-PCNPs (F11, F21 and F31) decomposed at 315–320 °C instead of 280 °C for pure 5-FU which was attributed to the presence of PCL that increased the thermal stability of 5-FU–PCNPs compared to pure 5-FU and PCNPs [54]. Both of PCNPs and 5-FU–PCNPs showed low thermal stability compared to pure PCL which was referred to the fact that the nanoparticles have a greater superficial area with higher reactivity than the polymer which led to faster thermal decomposition. A similar observation was noted in the literature [52] which confirmed the results obtained from XRD.

TEM

TEM images of the prepared nanoparticle formulations (F11, F21 and F31) are shown in Fig. 9, which reveals shape and size of the nanoparticles. It is clear from the TEM images that F31 nanoparticles have smaller size and spherical shape than that of F21 and F11. Figure 9 shows that F31 nanoparticles are spherical in the shape and appear well dispersed without agglomeration. However, the size of F21 nanoparticles is not spherical shape which may be due to aggregation of nanoparticles. Also, Fig. 9 shows that F11 nanoparticles have large size of F11 nanoparticles may be due to the loading of 5-FU into PCL shell nanoparticles expands the size of

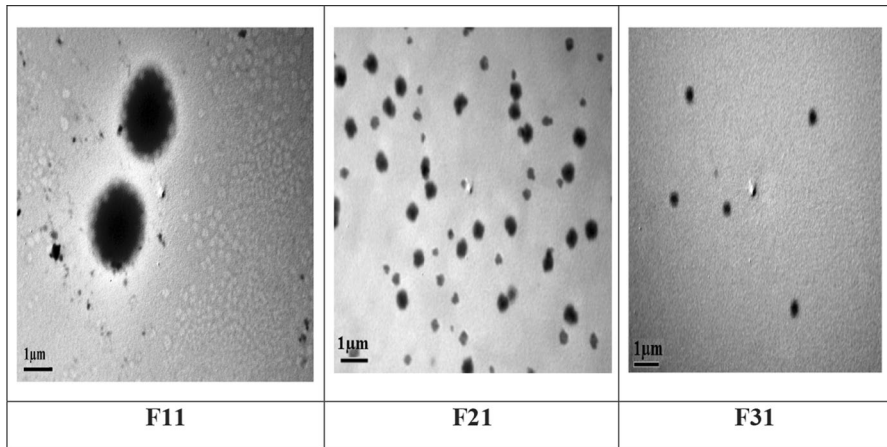


Fig. 9 TEM images of F11, F21 and F31 nanoparticle formulations

nanoparticles. It was observed that the encapsulation of 5-FU as a faint thin layer visible at the inner core of the nanoparticles.

SEM

SEM was used to determine the surface morphology of some samples of 5-FU–PCNPs as F35, F31, F21 and blank PCNPs (F_B) (PCNPs without using of 5-FU) as presented in Fig. 10. SEM images presented that all nanoparticles have smooth a spherical surfaces with and absolutely thin distribution size. The particles were slightly smaller, and some particles had pores on their surfaces due to the shrinkage expected by drying during the dichloromethane evaporation. Some of the particles were also bound together due to the surface tension of water on the particles during dehydration, as determined by Wu and Clark [55]. So the contact between the particles is attributed to the presence of traces of PVA, which were not easily removed due to the adhesive nature of PVA [41]. These images show that all the particles have a spherical shape. From the interpretations of the SEM images, it was found that the particles obtained with a concentration of 3% PCL (F31) had a narrow size distribution and a more ordered shape compared to the particles obtained from the concentration of 2% PCL (F21) as shown in Fig. 10. This corresponds to, moreover, the polymer concentration contains an important factor affecting the properties of PCNPs prepared according to the double emulsification technique according to the literature [31]. Moreover, two samples were prepared with PVA concentration of 0.5% and 1% in the external water phase and its effect on morphology was studied with SEM. From the SEM images, it was evident that the particles prepared with 0.5% PVA (F35) showed good morphology with a smooth, ordered shape compared to the particles prepared with 1% PVA (F31), which were grouped together as shown in Fig. 10. This clumping may be due to excessive PVA which leads to macromolecule adhesion through dehydration.

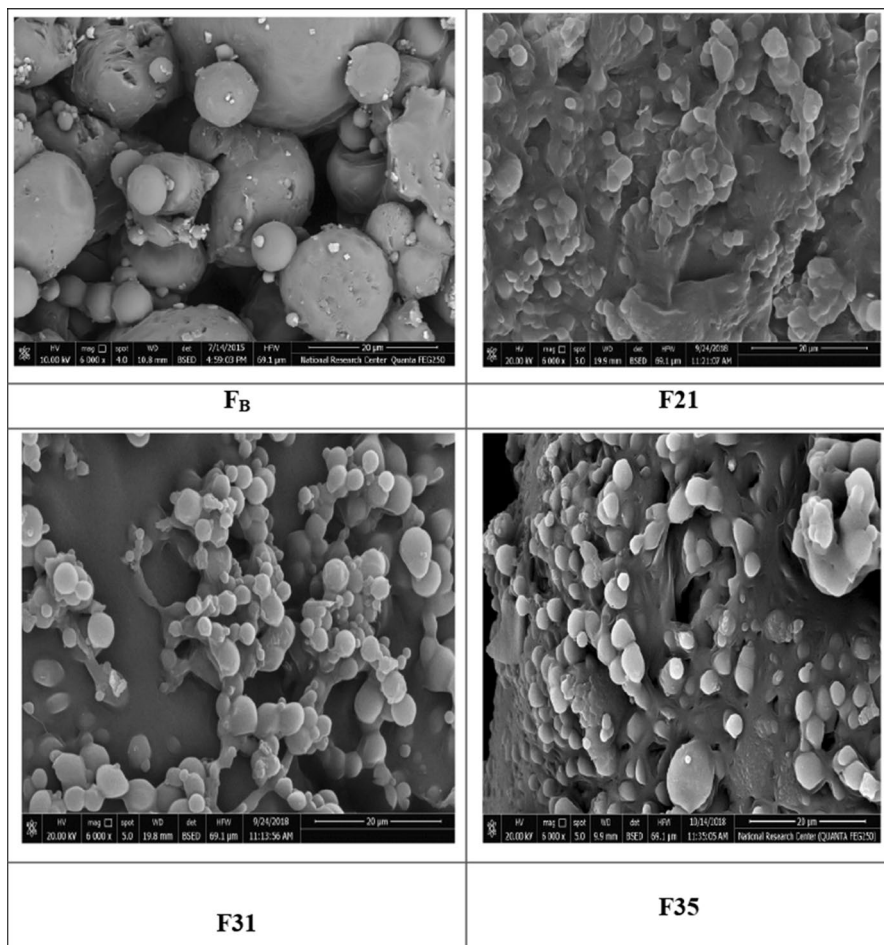


Fig. 10 SEM images of samples blank PCNPs (drug free, FB), 5-FU-PCNPs for F21, F31, F35 at magnification of 6000x

DLS comparative study of nanoparticles

Aqueous solutions of the studied samples were not molecularly dispersed. There were two types of particles with hydrodynamic radii R_m (middle mode) and R_s (slow mode). It may be assumed that the scattering objects responsible for the middle and slow modes are micelle-like structures and large aggregates. The hydrodynamic radii decreased with dilution (Fig. 11) that possibly caused by as a minimum two reasons. Firstly, this can be explained by the concentration need of the diffusion coefficient DO . Second, with the increase in concentration, we can imagine a growth in the real size of the micelles and collections. Extrapolations of the R_m and R_s values to zero concentrations give close values for samples with different compositions: The hydrodynamic radius of micelles is $R_m = (24 \pm 3)$, nm and the hydrodynamic radius

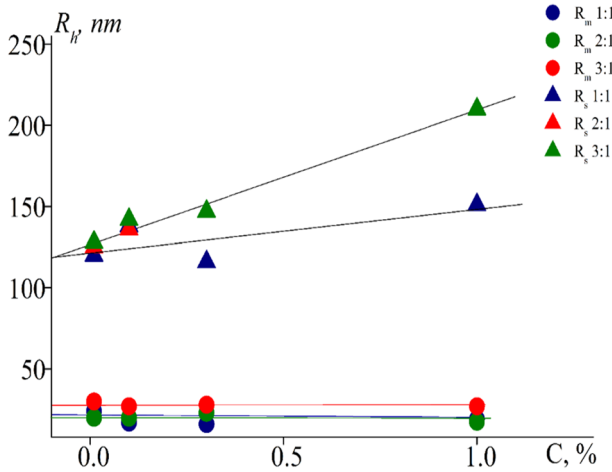


Fig. 11 Concentration dependences of hydrodynamic radii of scattering objects

of aggregates is $R_s = (120 \pm 10)$ nm. Thus, the sample composition does not affect the size of the supramolecular structures formed in solutions. For all the solutions studied, the contribution of micelle-like structures S_m to the total light scattering is small; it is much smaller than the contribution S_s of large aggregates in (Tables 3, 4, 5). However, the actual ratio of different types of particles in solutions is different. The relative weight fractions of micelles c_m and aggregates c_s in solutions were estimated using experimental values of R_m , R_s , S_m and S_s . According to the static light scattering theory, the intensity I is proportional to both the molar mass M and concentration c of particles, i.e., $I \sim cM$. The particle radius R is related to its molar mass as $M \sim Rx$, where parameter x depends on the particle shape: $x=2$ for coil and $x=3$ for rigid sphere. The values of c_m and c_s obtained with models coil (micelle)/coil (aggregate) and sphere (micelle)/coil (aggregate) are presented in Tables 3, 4, 5. One can see that micelle-like structures prevail in investigated solutions. The most important is that the composition of the dissolved particles does not change at passage transition from sample to sample. Aqueous solutions of the studied samples

Table 3 DLS results for the dilute aqueous solutions of F11 nanoparticle formulation

F11								
c	$R_m, \text{ nm}$	$R_s, \text{ nm}$	S_m	S_s	c_m	c_s	c_m	c_s
1	19	151	1	99	0.61	0.39	0.97	0.03
0.3	16	116	1	99	0.65	0.35	0.97	0.03
0.1	17	138	2	98	0.43	0.57	0.93	0.07
0.01	24	120	2	98	0.66	0.34	0.98	0.02
average					0.59		0.96	
used molecular model					<i>coil/coil</i>		<i>sphere/coil</i>	

Table 4 DLS results for the dilute aqueous solutions of F21 nanoparticle formulation

F21								
c	R_m , nm	R_s , nm	S_m	S_s	c_m	c_s	c_m	c_s
1	17.5	210	1	99	0.41	0.59	0.92	0.08
0.3	23	147	0.5	99.5	0.83	0.17	0.99	0.01
0.1	20	136	1	99	0.68	0.32	0.98	0.02
0.01	20	125	1	99	0.72	0.28	0.98	0.02
<i>average</i>					0.66		0.97	
<i>used molecular model</i>					<i>coil/coil</i>		<i>sphere/coil</i>	

Table 5 DLS results for the dilute aqueous solutions of F31 nanoparticle formulation

F31								
c	R_m , nm	R_s , nm	S_m	S_s	c_m	c_s	c_m	c_s
1	27	210	1	99	0.62	0.38	0.98	0.02
0.3	28	147	1	99	0.78	0.22	0.99	0.01
0.1	27	142	1.5	98.5	0.70	0.30	0.98	0.02
0.01	30	128	4.8	95.2	0.52	0.48	0.97	0.03
<i>average</i>					0.66		0.98	
<i>used molecular model</i>					<i>coil/coil</i>		<i>sphere/coil</i>	

were not molecularly dispersed; there were two types of particles, namely micelle-like structures and large aggregates. The sample composition does not affect the size of the supramolecular structures formed in aqueous solutions under study. The composition of the scattering objects does not depend on the component ratio in the sample.

Drug release behavior

The percentage of released 5-FU from the samples was investigated by UV–Vis spectrophotometer. Maximum absorbance of the 5-FU in PBS was obtained at 266.4 nm by spectrophotometer [40]. Figure 12 displays in vitro drug release in vitro release profile for 5-FU from three selected PCNPs; F11, F21 and F31 compared to the free 5-FU suspension. The three formulations (i.e., F11, F21, and F31) have high EE% values of 30.5, 29 and 40.7%, respectively. All three PCNPs demonstrated a sustained release profile in which the 5-FU percentage released after 48 h was 34.17%, 25.51% and 20.01% for F11, F21 and F31, respectively. On the other hands, the 5-FU suspension showed a very fast release, reaching 91.32% after just six hours. The release profiles of the examined PCNPs showed biphasic behavior, with an early rapid release detected within the first hour. This was followed by a slow and sustained release that lasted up to 48 h. The slow release behavior of 5-FU from PCL

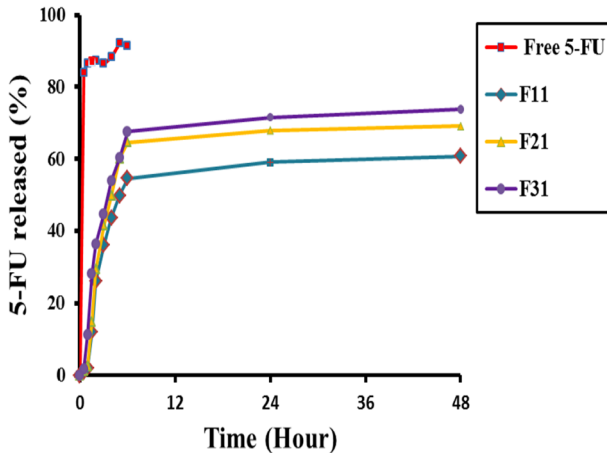


Fig. 12 In vitro release profiles of free 5-FU and PCNPs formulations (F11, F21 and F31) in phosphate buffer, pH 7.4

as carriers [45, 56] was previously reported and could be due to the strong hydrogen bond between 5-FU molecules and PCL delaying 5-FU diffusion in the release medium. Another important note is that after 48 h, the percentage of drug released was significantly increased ($P < 0.05$) as the PCL concentration increased, and the percentage of drug released at a colonic pH of 7.4 decreased. Indeed, increasing the PCL concentration from 1 to 3% reduced the fraction of the released drug at pH 7.4 from 60.3 to 40.9% after 28 h. This may be the amorphous nature of PCL (seen in both formulations as F11, F21 and F31 from Fig. 12), which would accelerate decomposition. The used PCL $M_w = 14,000$ g/mol, it is a very clearly observed phenomenon that the release mechanism can easily be modulated by the weight of used polymer as higher molecular weight polymer shows slower release of the drugs [57]. It has been observed that at the same amount of polymer in the microspherical system, the polymers of higher viscosity are difficult to dissolve. The main reason behind this phenomenon is the requirement of higher energy to pull the chain of polymers of higher viscosity from their matrix and formation of thicker gel layer after the hydration. The viscosity effect is mainly due to the differences in the molecular weight of the polymers. The following equation has been derived to explain the relation between the polymer molecular weight and disentanglement concentration [58]:

Anticancer screening

Six different preparations were investigated in vitro for their behavior on human cancer cells as HCT-116, MCF-7, HepG2 and A549 in addition to on human normal cells RPE-1 using the MTT assay. The percentages of intact cells were calculated and compared with those in the control. The effect of these preparations against four cancer cell strains lines compared with the activity of doxorubicin in addition to its activity on normal cells. All preparations suppressed the five human cells in a dose-dependent manner (Figs. 13, 14, 15, 16, 17). In order to study the efficacy and safety

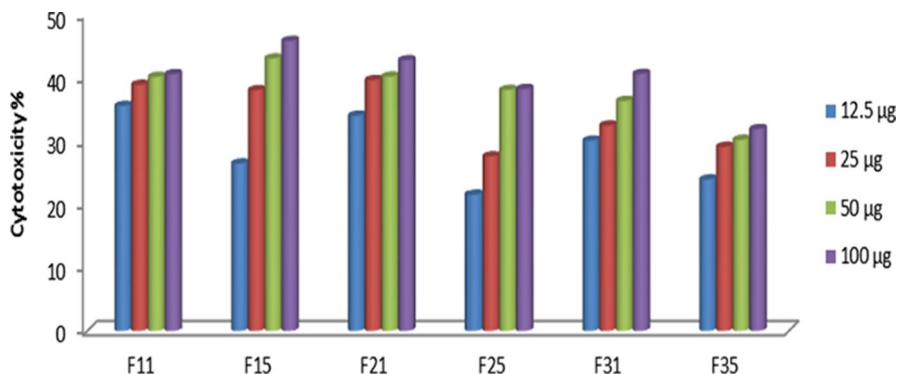


Fig. 13 Dose dependent cytotoxic activities of six preparations against HCT-116 cancer cells using MTT assay

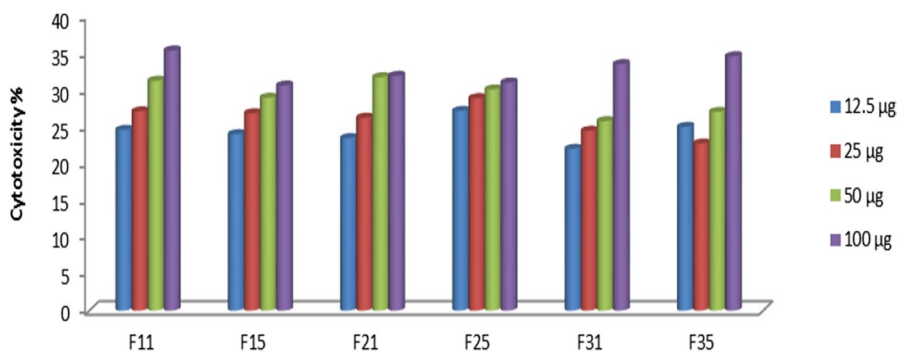


Fig. 14 Dose-dependent cytotoxic activities of six preparations against A549 cancer cells using MTT assay

of the six preparations, the cytotoxic effect of all formulation was related to the cytotoxicity of the reference drug (doxorubicin) as follows. In case of HCT-116, MCF-7, HepG2, A549 and RPE-1, both Figs. 13, 14, 15, 16, 17 and Table 6 show that all six formulations are significantly less cytotoxic compared to doxorubicin. All the six preparations considered safe to be used on both cancer and normal human cells. In conclusion, due to the safety effect, these six preparations could be used as effective drug carriers to deliver drugs without any toxic effect on the healthy cells.

Conclusion

5-FU-PCNPs were prepared by double emulsion method in which a number of factors affecting particle size such as the PCL concentration for first emulsion and concentration PVA for second emulsion were examined. An increase in observed of the EE% values with increasing concentration of PCL from 1 to 3%. Also, increase in

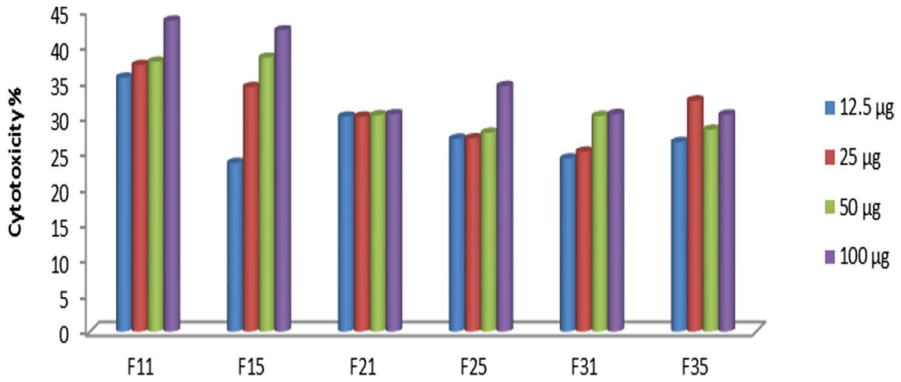


Fig. 15 Dose-dependent cytotoxic activities of six preparations against MCF-7 cancer cells using MTT assay

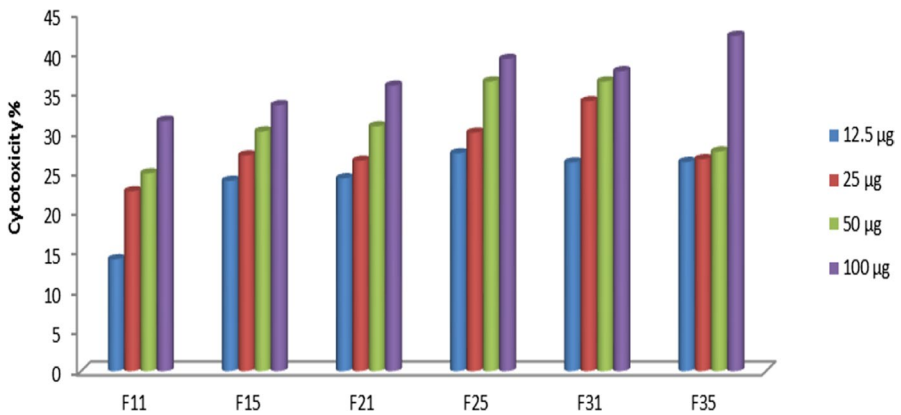


Fig. 16 Dose-dependent cytotoxic activities of six preparations against HepG2 cancer cells using MTT assay

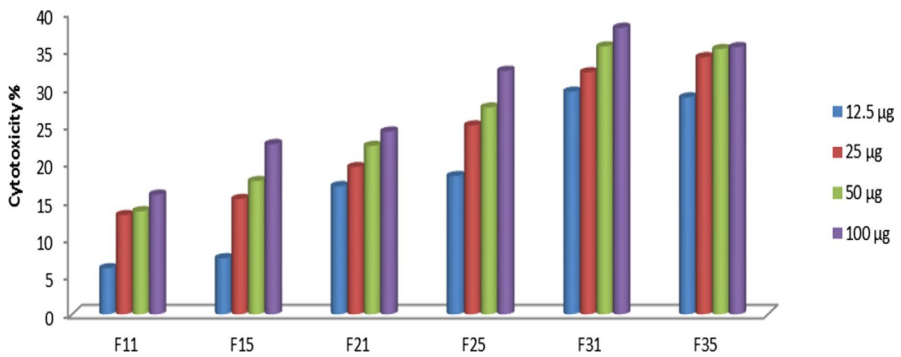


Fig. 17 Dose-dependent cytotoxic activities of six preparations against RPE-1 normal cells using MTT assay

Table 6 Cytotoxic activities IC₅₀ values of the obtained preparations using MTT assay against the four cancer cell type and one healthy type

Compound	IC ₅₀ (µg/mL) ± SD				
	HCT-116	A549	MCF-7	HepG2	RPE-1
F11	63.4 ± 5.1	87.6 ± 5.3	90.9 ± 4.5	80.6 ± 5.1	127.5 ± 6.9
F15	64.3 ± 4.5	91.0 ± 5.1	72.1 ± 4.2	72.6 ± 4.9	117.1 ± 5.9
F21	63.0 ± 4.9	89.8 ± 4.9	70.6 ± 4.4	71.8 ± 4.5	104.2 ± 5.7
F25	73.4 ± 4.9	87.8 ± 4.9	89.4 ± 4.5	67.1 ± 4.3	93.9 ± 4.9
F31	68.4 ± 5.1	93.4 ± 5.5	78.5 ± 4.2	66.7 ± 3.9	79.6 ± 4.9
F35	76.5 ± 5.3	91.7 ± 5.2	89.7 ± 5.3	70.1 ± 4.4	80.4 ± 4.8
Doxorubicin	23.2 ± 3.9	33.7 ± 4.1	37.6 ± 4.1	14.3 ± 2.5	37.1 ± 3.4

EE% values was observed with increasing concentration of PVA of second emulsion from 1 to 3% at constant concentration of PCL of first emulsion. PCL concentration has an important effect on particle size, that is, the particle size increases relatively when the amount of PCL is increased, while at low PVA concentration, a smaller particle size could be achieved than at higher concentration. From the SEM images, it was representing that the surface morphology of the obtained nanoparticles has a smooth surface with spherical shape. The XRD study revealed the molecularly dispersed 5-FU in nanoparticles in the case of 5-FU-loaded nanoparticles. Finally, correlations between structural and morphological factors and preparation conditions (composition, concentration of stabilizer) were evaluated. Estimation of the efficacy of 5-FU drug encapsulation in the polymer matrix showed that the prepared polycaprolactone nanoparticles be used effectively for the preparation of controlled release matrices for anticancer drug. All six formulations were significantly less cytotoxic than the reference drug (doxorubicin). All six formulations are safe to use on both cancer cells and normal human cells.

Author contributions MS was involved in conceptualization, methodology, investigation, resources, data curation, writing—reviewing and editing. HMA contributed to methodology, visualization, conducted the biological assays and provided the experimental procedures and results of biological part. MMHA was involved in conceptualization, methodology, writing—reviewing and editing, visualization, funding acquisition.

Declarations

Conflict of interest The authors report no declarations of interest.

References

1. Wang MD, Shin DM, Simons JW, Nie S (2007) Nanotechnology for targeted cancer therapy. *Expert Rev Anticancer Ther* 7:833–837

2. Nie S, Xing Y, Kim GJ et al (2007) Nanotechnology applications in cancer. *Annu Rev Biomed Eng* 9:257–288
3. Youan BB (2008) Impact of nanoscience and nanotechnology on controlled drug Delivery. *Nano-medicine* 3:401–406
4. Farokhzad OC, Langer R (2009) Impact of nanotechnology on drug delivery. *ACS Nano* 3:16–20
5. Peer D, Karp JM, Hong S et al (2007) Nanocarriers as an emerging platform for cancer therapy. *Nat Nanotechnol* 2:751–760
6. Cho K, Wang X, Nie S et al (2008) Therapeutic nanoparticles for drug delivery in cancer. *Clin Cancer Res* 14:1310–1316
7. Salerno A, Domingo C, Saurina J (2017) PCL foamed scaffolds loaded with 5-fluorouracil anti-cancer drug prepared by an eco-friendly route. *Mater Sci Eng C Mater Biol Appl* 75:1191–1197
8. Nivethaa EAK, Dhanavel S, Rebekah A, Narayanan V, Stephen A (2016) A comparative study of 5-Fluorouracil release from chitosan/silver and chitosan/silver/MWCNT nanocomposites and their cytotoxicity towards MCF-7. *Mater Sci Eng C Mater Biol Appl* 66:244–250
9. Tummala S, Satish Kumar MN, Prakash A (2015) Formulation and characterization of 5- fluorouracil enteric coated nanoparticles for sustained and localized release in treating colorectal cancer. *Saudi Pharm J* 23(3):308–314
10. S Rossi, ed. *Australian Medicines Handbook* (2013 ed.). Adelaide: The Australian Medicines Handbook Unit Trust, 2013
11. World Health Organization (WHO) Model list of essential medicines. World Health Organization; October 2013. Accessed April 22, 2014
12. Arias JL (2008) Novel strategies to improve the anticancer action of 5-fluorouracil by using drug delivery systems. *Molecules* 13(10):2340–2369
13. Sun L, Chen Y, Zhou Y, Guo D, Fan Y, Guo F, Zheng Y, Chen W (2017) Preparation of 5- fluorouracil-loaded chitosan nanoparticles and study of the sustained release in vitro and in vivo. *Asian J Pharm Sci* 12(5):418–423
14. Zhang N, Yin Y, Xu SJ et al (2008) 5-Fluorouracil: mechanisms of resistance and reversal strategies. *Molecules* 13:1551–1569
15. Arias JL, Ruiz MA, López-Viota M et al (2008) Poly(alkylcyanoacrylate) colloidal particles as vehicles for antitumour drug delivery: a comparative study. *Colloids Surf B* 62:64–70
16. Zhang N, Yin Y, Xu SJ, Chen WS (2008) 5-Fluorouracil: mechanisms of resistance and reversal strategies. *Molecules* 13(8):1551–1569
17. Arias JL, Ruiz MA, Lopez-Viota M, Delgado AV (2008) Poly(alkylcyanoacrylate) colloidal particles as vehicles for antitumour drug delivery: a comparative study. *Colloids Surf B: Biointerfaces* 62(1):64–70
18. Sahle FF, Balzus B, Gerecke C, Kleuser B, Bodmeier R (2016) Formulation and in vitro evaluation of polymeric enteric nanoparticles as dermal carriers with pH dependent targeting potential. *Eur J Pharm Sci* 92:98–109
19. Matsumura Y, Maeda H (1986) A new concept for macromolecular therapeutics in cancer chemotherapy: mechanism of tumortropic accumulation of proteins and the antitumor agent smancs. *Cancer Res* 46:6387–6392
20. Mora-Huertas CE, Fessi H, Elaissari A (2010) Polymer-based nanocapsules for drug delivery. *Int J Pharm* 385(1):113–142
21. Kumar P, Gajbhiye KR, Paknikar KM, Gajbhiye V (2019) Current status and future challenges of various polymers as cancer therapeutics. In: Kesharwani P, Paknikar KM, Gajbhiye V (eds) *Polymeric Nanoparticles as a Promising Tool for Anti-Cancer Therapeutics*. Academic Press, United states
22. Amin A, Samy M, Abd El-Alim SH, Rabia AEG, Ayoub MMH (2018) Assessment of formulation parameters needed for successful vitamin C entrapped polycaprolactone nanoparticles. *Int J Polym Mater Polym Biomater* 67(16):942–950
23. Othman R, Vladisavljević GT, Nagy ZK (2015) Preparation of biodegradable polymeric nanoparticles for pharmaceutical applications using glass capillary microfluidics. *Chem Eng Sci* 137:119–130
24. Wang S, Chen H, Cai Q, Bei J (2001) Degradation and 5-fluorouracil release behavior in vitro of polycaprolactone/poly(ethylene oxide)/polylactide tri-component copolymer†1. *Polym Adv Technol* 12(3–4):253–258
25. Sastre RL, Blanco MD, Teji3n C, Olmo R, Teji3n JM (2004) Preparation and characterization of 5-fluorouracil-loaded poly(ϵ -caprolactone) microspheres for drug administration. *Drug Dev Res* 63(2):41–53

26. Canfarotta F, Whitcombe MJ, Piletsky SA (2013) Polymeric nanoparticles for optical sensing. *Bio-technol Adv* 31:1585–1599
27. Huang S-H, Hsu T-T, Huang T-H, Lin C-Y, Shie M-Y (2017) Fabrication and characterization of polycaprolactone and tricalcium phosphate composites for tissue engineering applications. *J Dental Sci* 12:33–43
28. Ayoub M, Ahmed N, Kalaji N, Charcosset C, Magdy A, Fessi H, Elaissari A (2011) Study of the effect of formulation parameters/variables to control the nanoencapsulation of hydrophilic drug via double emulsion technique. *J Biomed Nanotechnol* 7:255–262
29. Amin A, Samy M, Abd El-Alim SH, Rabia AG, Ayoub MMH (2018) Assessment of formulation parameters needed for successful vitamin C entrapped polycaprolactone nanoparticles. *Int J Polym Mater Polym Biomater* 67:942–950
30. Iqbal M, Zafar N, Fessi H, Elaissari A (2015) Double emulsion solvent evaporation techniques used for drug encapsulation. *Int J Pharm* 496:173–190
31. Samy M, Abdallah HM, Ayoub MMH, Vylegzhanina ME, Volkov AY, Sukhanova TE (2020) Eco-friendly route for encapsulation of 5-fluorouracil into polycaprolactone nanoparticles. *Egypt J Chem* 63:255–267
32. Hassan AS, Mady MF, Awad HM, Hafez TS (2017) Synthesis and antitumor activity of some new pyrazolo [1, 5-a] pyrimidines. *Chinese Chem Lett* 28(2):388–393. <https://doi.org/10.1016/j.ccl.2016.10.022>
33. Emam AN, Loutfy SA, Mostafa AA, Awad HM, Mohamed MB (2017) Cyto-toxicity, biocompatibility and cellular response of carbon dots–plasmonic based nano-hybrids for bioimaging. *RSC Adv* 7:23502–23514
34. Flefel EM, El-Sayed WA, Mohamed A M, El-Sofany WI, Awad HM (2017) Synthesis and anticancer activity of new 1-Thia-4-azaspiro [4.5] decane, their derived thiazolopyrimidine and 1,3,4-thiadiazole thioglycosides. *Molecules* 22(170):1–13
35. Zamora-Mora V, Fernández-Gutiérrez M, González-Gómez Á, Sanz B, Román JS, Goya GF, Hernández R, Mijangos C (2017) Chitosan nanoparticles for combined drug delivery and magnetic hyperthermia: from preparation to in vitro studies. *Carbohydr Polym* 157:361–370
36. Salar RK, Kumar N (2016) Synthesis and characterization of vincristine loaded folic acid–chitosan conjugated nanoparticles. *Resour-Effic Technol* 2(4):199–214
37. Badran MM, Mady MM, Ghannam MM, Shakeel F (2017) Preparation and characterization of polymeric nanoparticles surface modified with chitosan for target treatment of colorectal cancer. *Int J Biol Macromol* 95:643–649
38. Khoe S, Kardani M (2014) Preparation of PCL/PEG superporous hydrogel containing drug-loaded nanoparticles: the effect of hydrophobic–hydrophilic interface on the physical properties. *M Eur Polym J* 58:180–190
39. Aydin RST, Pulat M (2012) 5-fluorouracil encapsulated chitosan nanoparticles for pH-stimulated drug delivery: evaluation of controlled release kinetics. *J Nanomater* 2012:42
40. Samy M, Abd El-Alim SH, Rabia AG, Amin A, Ayoub MMH (2020) Formulation, characterization and in vitro release study of 5-fluorouracil loaded chitosan nanoparticles. *Int J Biol Macromol* 156:783–791
41. Ibraheem D, Iqbal M, Agusti G, Fessi H, Elaissari A (2014) Effects of process parameters on the colloidal properties of polycaprolactone microparticles prepared by double emulsion like process. *Colloids Surf A: Physicochem Eng Aspects* 445:79–91
42. Guo Y, Halaev ES, Smith S (2013) Physical stability of pharmaceutical formulations: solid-state characterization of amorphous dispersions: review. *Trends Anal Chem* 49:137–144
43. Singh M, Hagan DO (1998) The preparation and characterization of polymeric antigen delivery systems for oral administration. *Adv Drug Delivery Rev* 34:285–304
44. Prieto C, Calvo LJ (2017) Supercritical fluid extraction of emulsions to nanoencapsulate vitamin E in polycaprolactone. *J. Supercrit Fluids* 119:274–282
45. Ortiz R, Prados J, Melguizo C, Arias JL, Adolfiná Ruiz M, Álvarez JP, Caba O, Luque R, Segura A, Aránega A (2012) 5-Fluorouracil-loaded poly(ϵ -caprolactone) nanoparticles combined with phage E gene therapy as a new strategy against colon cancer. *Int J Nanomedicine* 7:95–107
46. Öztürk K, Mashal AR, Yegin BA, Çaliş S (2015) Preparation and in vitro evaluation of 5-fluorouracil-loaded PCL nanoparticles for colon cancer treatment. *Pharm Dev Technol*. <https://doi.org/10.3109/10837450.2015.1116565>
47. Babu PK, Maruthi Y, Pratap SV, Sudhakar K, Sadihu R, Prabhakar MN, Song JI, Subha MCS, Rao KC (2015) Development and characterization of polycaprolactone (PCL)/

- Poly((R)-3-hydroxybutyric acid)(PHB) blend microspheres for tamoxifen DRUG release studies. *Int J Pharm Pharm Sci* 7(9):95–100
48. Katakam P, Phalguni Y, Harinarayana D (2014) Formulation, characterization and in vitro evaluation of capecitabine loaded polycaprolactone-chitosan nanospheres. *Bangladesh Pharm J* 17:18–24
 49. Li P, Wang Y, Peng Z, P Li, Wang Y, Peng Z, She MF, Kong L (2010) Physicochemical property and morphology of 5-fluorouracil loaded chitosan nanoparticles. *International Conference on Nanoscience and Nanotechnology*
 50. Ashour AE, Badran M, Kumar A, Hussain T, Alsarra IA, Yassin AEB (2019) Physical pegylation enhances the cytotoxicity of 5-fluorouracil-loaded PLGA and PCL nanoparticle. *Int J Nanomedicine* 14:9259–9273
 51. Yang H, Irudayaraj J (2002) Rapid determination of vitamin C by NIR, MIR and FT- raman techniques. *J Pharm Pharmacol* 54:1247–1255
 52. Guirguis OW, Moselhey MTH (2012) Thermal and structural studies of poly (vinyl alcohol) and hydroxypropyl cellulose blends. *Nat Sci* 4:57–67
 53. Fukushima K, Tabuani D, Camino G (2009) Nanocomposites of PLA and PCL based on montmorillonite and sepiolite. *Mater Sci Eng C* 29:1433–1441
 54. Jagadeesh HG, Kusmdevi V (2010) Tamoxifen loaded poly (ε-caprolactone) based injectable microspheres for breast cancer. *Int J Pharm Pharm Sci* 2(4):189–195
 55. Wu Y, Clark RL (2007) Controllable porous polymer particles generated by electrospraying. *J Colloid Interface Sci* 310:529–535
 56. Iqbal S, Rashid MH, Arbab AS, Khan M (2017) Encapsulation of anticancer drugs (5-Fluorouracil and Paclitaxel) into polycaprolactone (PCL) nanofibers and in vitro testing for sustained and targeted therapy. *J Biomed Nanotechnol* 13(4):355–366
 57. Kumari A, Yadav SK, Yadav SC (2010) Biodegradable polymeric nanoparticles based drug delivery systems. *Colloids Surf B Biointerfaces* 75(1):1–18
 58. Heng PW, Chan LW, Easterbrook MG, Li X (2001) Investigation of the influence of mean HPMC particle size and number of polymer particles on the release of aspirin from swellable hydrophilic matrix tablets. *J Control Release* 76(1–2):39–49

Publisher's Note Springer Nature remains neutral with regard to jurisdictional claims in published maps and institutional affiliations.